THERMALIZED AND REACCELERATED BEAMS AT THE NATIONAL SUPERCONDUCTING CYCLOTRON LABORATORY

S. J. Williams[*], T. M. Baumann, K. Cooper, A. Lapierre, D. Leitner, D. J. Morrissey,
J. A. Rodriguez, S. Schwarz, A. Spyrou, M. Steiner, C. Sumithrarachchi, W. Wittmer,
NSCL, Michigan State University, 640 S. Shaw Lane, East Lansing, MI 48824, USA
G. Perdikakis, Central Michigan University, Mt. Pleasant, MI 48859, USA

Abstract

The National Superconducting Cyclotron Laboratory at Michigan State University is a Rare Isotope Beam (RIB) facility providing beams of exotic nuclear species through projectile fragmentation. The Coupled Cyclotron Facility accelerates stable ion beams to ∼100 MeV/A which are then fragmented and selected with the A1900 separator. A recent addition to NSCL is the gas stopping facility which thermalizes the high energy beam. The RIBs are extracted at ≤60 keV and selected by mass for further transport to the low energy areas, currently consisting of the BECOLA beam cooling and laser spectroscopy system, and LEBIT Penning trap. RIBs up to 12 MeV/A will be provided by the ReA post-accelerator, comprising of an EBIT, RFQ and superconducting RF cavities. Energies up to 2.4 MeV/A for certain species are presently available, and energy increases will be phased in with the addition of further cryomodules. In a campaign of commissioning experiments, RIBs from a fragmentation facility were thermalized and post-accelerated for the first time.

INTRODUCTION

At the forefront of current nuclear physics research is the drive to understand emerging phenomena observed in regions of the nuclear chart away from the valley of beta-stability. As the isospin degree of freedom is explored, new information on the evolution of shell structure, the observation of exotic structures and the understanding of stellar evolution and nucleosynthesis is made available and possible. The primary tool for this research is the exploitation of rare isotope beams. The National Superconducting Cyclotron Laboratory (NSCL) is currently undergoing an expansion of its capablilities with the commissioning of beam thermalization and post-acceleration facilities, which will provide RIBs at energies up to 12 MeV/A [1]. The beams are produced through fast fragmentation of high energy (∼100 MeV/A) stable beams provided by the Coupled Cyclotron Facility[2], which by 2022 will be replaced with the Facility for Rare Isotope Beams (FRIB)[3], a 400 kW superconducting heavy-ion driver linac providing up to three orders of magnitude more primary beam power. In the current facility the secondary fragments are separated achromatically in the A1900 separator [4] and the se-

lected isotope transported to the beam thermalization area where it is slowed and extracted in a He gas cell [5, 6]. Following extraction at ≤60 keV the beam is transported to a 0.75 Tesla LEBT dipole magnet for mass selection, and further to the LEBIT Penning trap for high precision mass measurements, the BECOLA beam cooling and laser spectroscopy system, or the ReA post-accelerator. This paper reports upon the first post-acceleration of thermalized fragmentation rare isotope beams at NSCL and the beam diagnostics challenges associated with the process.

DIAGNOSTICS FOR RARE ISOTOPE BEAMS

The challenges faced by diagnostics for rare isotope beams at NSCL are associated with the varying environments in which they must be deployed. The secondary fragment cocktail is usually of the order of ∼80 MeV/A and can be at rates approaching 10^7 pps. The thermalization in the gas cell is tuned to a particular fragment by the use of a variable-angle wedge degrader, but ionization processes cause the creation of weakly bound molecules from residual gas elements which are extracted at ≤60 keV along with the rare isotope beam. Here the challenge is to detect the presence of the rare isotope beam in a background of stable molecules at currents of a few tens of picoamps. In addition, depending on the chemical nature of the rare isotope beam its intensity may be distributed amongst a number of molecules. Diagnostics must be able to simultaneously detect the stable and radioactive currents to support the selectivity of the LEBT dipole and ensure a single species is transported further. For post-acceleration the selected beam is injected into an Electron Beam Ion Trap (EBIT) [7] for breeding to charge states suitable for injection into the ReA Radio Frequency Quadrupole (RFQ). Following charge breeding an achromatic charge-over-mass (Q/A) separator is used to select the rare isotope beam at a particular charge state. This Q/A value may overlap with that of stable residual gas elements and diagnostics are required to select the region in the Q/A landscape that corresponds to an acceptable compromise between purity and intensity of the rare isotope of interest. Each of these situations is discussed in the context of the two experiments that are reported upon in this paper.

_____
[*] WilliaSc@nscl.msu.edu

GALLIUM-76

For the first commissioning and proof-of-principle experiment ^{76}Ga (T$_{\frac{1}{2}}$=32.6s) was produced from a ^{76}Ge primary beam at an energy of 130 MeV/A. This reaction, involving neutron pickup, was selected due to the significantly enhanced purity offered compared to other options using standard fragmentation of heavier beams, with the trade-off of reduced rate. In order to identify the contents of the high energy beam transported to the entrance of the gas cell, a 300μm silicon PIN detector is inserted into the beam. The beam energy is measured using a Mesytec MSCF-16 shaping amplifier and CAEN V785 ADC, and its time-of-flight with respect to the cyclotron RF measured in a CAEN V775 TDC following fast pickoff with a Canberra 454 TDC. In this configuration the silicon detector is in energy loss mode. Figure 1 shows a two dimensional particle identification plot of time-of-flight versus energy loss. From this figure the favourable conditions for such a commissioning experiment are clear, as only two species are transported to the gas cell. For this setting, ^{76}Ga has a purity of around 80%.
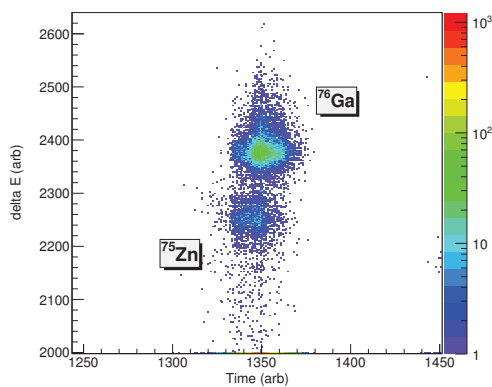

Figure 1: Particle identification plot of time-of-flight versus energy loss in an in-beam silicon detector for the ^{76}Ga experiment. Around 80% of the counts observed fall within the ^{76}Ga locus.

This beam was thermalized in and extracted from the gas cell, charge-bred in the EBIT and accelerated to 1.0 MeV/A in ReA. Count rates of a few per minute were observed following acceleration, confirming the proof-of-principle operation of the post-accelerated rare isotope beams at NSCL. The following sections discuss a follow-up experiment with a ^{37}K beam, which was optimized for higher production rates.

POTASSIUM-37

To produce ^{37}K (T$_{\frac{1}{2}}$=1.23s), a primary beam of ^{40}Ca at 140 MeV/A was fragmented and ^{37}K was selected for transport to the beam thermalization area. Following thermalization in the gas cell, in order to simultaneously observe stable beam currents and activity following radioac-

tive decay of RIBs the beam is impinged on to a series of decay counters. Figure 2 shows a number of three dimensional views of this diagnostics device. The rightmost panel of Fig. 2 shows a full view. The assembly is actuated into the beam by means of a pneumatic cylinder mounted to a CF flange, seen in the centre of this panel. The top left panel shows a detail view of the decay counter, where the beam enters from right to left. The foil indicated is 17μm aluminium, which is isolated from the body of the device, but in electical contact with the inner ring immediately adjacent to it. A contact is connected to a vacuum feedthrough which can be connected to a current integrating device, such that it can perform as a Faraday cup. The inner ring closest to the beam aperture is isolated from the cup assembly and is biased to 120V for secondary electron repulsion. The lower panel in Fig. 2 shows the same detail, but with the foil removed. As can be seen, a surface-barrier type silicon detector is mounted in electrical isolation behind the foil, and its microdot connector is connected to an isolated vacuum feedthrough for better noise performance. In this manner the device is simultaneously a faraday cup and radioactive decay counter, as when the implanted radioactive species decay, the resultant beta particles pass through the foil and deposit their energy in the silicon detector.
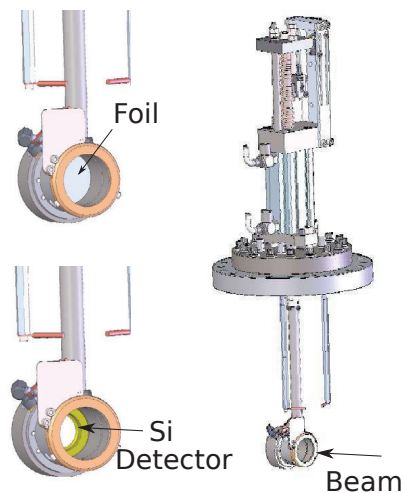

Figure 2: A three dimensional view of a decay counter. Rightmost panel: full view showing pneumatic actuator and detector assembly. Upper left panel: detail view of the decay counter showing stopping foil. Lower left panel: detail view of the decay counter with foil removed.

The energy in this detector is recorded on an event-by-event basis in the same data acquisition system as discussed earlier in this paper. In addition to the energy parameter, a Struck SIS3820 VME scaler is used to scale a clock, down-scaled from 50 MHz to a number appropriate to the experimental conditions (currently 10 kHz). The same clock is copied and vetoed by the system busy to generate a live and real clock. This allows the timestamping of each event and

significantly expands the utility of the decay counters.

Following extraction from the gas cell, the beam is transported through a 0.75T dipole magnet for mass selection. Using a Control System Studio application, the current in this magnet is scanned continuously over a range. At the exit of the magnet is another decay counter, which observes the selected mass. By correlating the field of the magnet with the event-by-event timestamp a mass scan can be performed that is only sensitive to the activity. Figure 3 shows the result of this scan for the ^{37}K beam. The favourable nature of the potassium chemistry is immediately evident with the observation that ~94% of the observed activity is found in one peak, corresponding to 37 atomic mass units. In addition, the ^{37}K is observed to exist in weakly bound molecular states with one to a few water ligands. By considering the possibility of doubly-charged ions, the peak at mass 37 is likely to consist of ^{37}K$^+$ and $[^{37}$K$(H_2O)_2]^{2+}$, at masses 37 and 36.5 respectively.
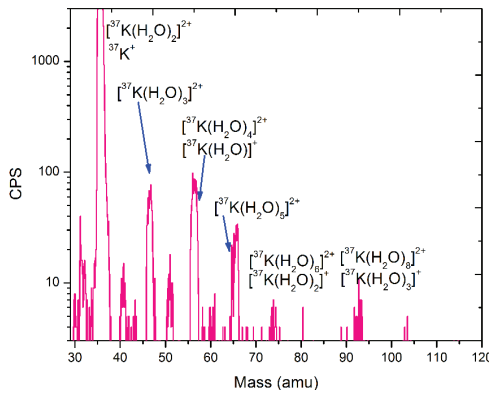

Figure 3: Activity scan of ^{37}K.

The selected mass was then injected into the ReA EBIT in a continuous beam. The EBIT breeds highly charged ions by confining the beam in electric and superconducting magnetic fields for tens of milliseconds where they overlap with a tightly focussed electron beam with a current of 750 mA. Repeated collisions breed the charge state of the injected beam from $[1,2]^+$ to Q^+ such that they reach the Q/A acceptance of the RFQ of 0.2 to 0.5. The Q+ ions are then ejected from the EBIT by lowering the confining potential at the entrance, and separated in an achromatic Q/A separator with both electric and magnetic sectors. Multiple charge states are possible upon ejection, the range of which is largely determined by the trap potential and the breeding time. In addition, even under vacuum conditions of $< 10^{-12}$ Torr, residual gases are charge bred at the same time as the rare isotope. Scanning the second, magnetic dipole, section of the Q/A separator and observing the current on a conventional Faraday cup results in Fig. 4. The dashed line in this figure corresponds to injection of stable ^{39} and was performed to investigate the charge breeding of potassium ions before the radioactive beam experiment.

The red labels indicate the expected locations of the ^{37}K$^{(16,17,18,19)+}$ ions and their overlaps with charge states
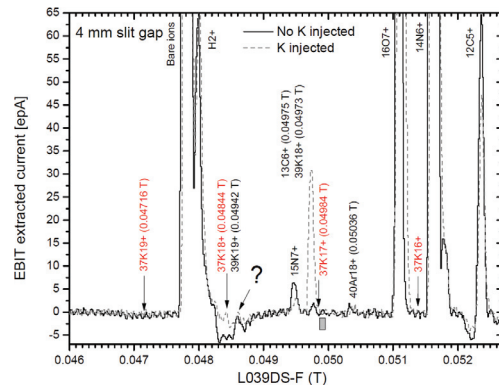

Figure 4: A Q/A scan of the region of interest for ^{37}K acceleration, showing the location of the (16-19)$^+$ charge states. These data were taken using a Faraday cup and a slit width of four millimetres.

of residual gas ions. From examination of this figure, it becomes obvious that the challenge is to find a region which has a low background. In addition, the observation of a current from a low intensity RIB is often below the limit of that achievable with a Faraday cup, and a method of single ion counting becomes essential.

For reasons that will be discussed in a later section, ^{37}K^{17+} was chosen for post-acceleration, and accelerated by the ReA accelerator to 2.4 MeV/A. In this commissioning experiment, ReA consisted of a multi-harmonic buncher, RFQ and two superconducting cryomodules, the first a solenoid and the second containing accelerating cavities. The acceleration of the beam to energies of a few MeV/A opens up the opportunity for more sensitive Q/A scans. By removing the foil from the decay counter (Fig. 2 lower left panel) the device provides a direct energy measurement of the impinging beam. Such a device was installed directly following the last cryomodule and thus saw the final beam energy. Measurement of the energy following acceleration in a linac corresponds to a direct measurement of the mass. Figure 5 shows a two dimensional plot of energy measured in the silicon detector (mass) versus Q/A as the magnetic sector of the Q/A section is scanned. For this measurement the slits following the dipole were set at one millimetre in order to highlight the separation capabilities of the Q/A section.

Figure 6 shows a projection of this matrix on to the y axis, which is the single-ion counting equivalent of Fig. 4, albeit with a much reduced range due to the acceptance of the RFQ. This spectrum shows excellent separation of the ^{13}C^{6+} from the peak corresponding to ^{37}(K,Cl)$^{17+}$, but doesn't, however, represent the beam quality observed during the experiment due to the size of the beam being larger than 1 mm at the exit of the magnet. For delivery to the experimental station, the slits were set at 3 mm to ensure the transport of all of the ^{37}K, with the known compromise of acceptance of contamination from ^{13}C^{6+}. ^{37}Cl is a stable contaminant due to residue from ultra high vacuum cleaning agents.
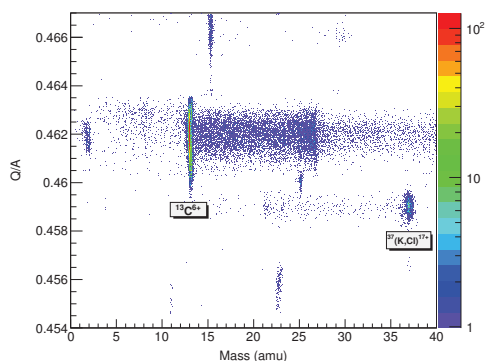
Figure 5: Two dimensional plot showing accelerated beam energy (mass) as a function of Q/A for the $^{37}K^{17+}$ region, as detected in an in-beam silicon detector using a slit width of one millimetre.
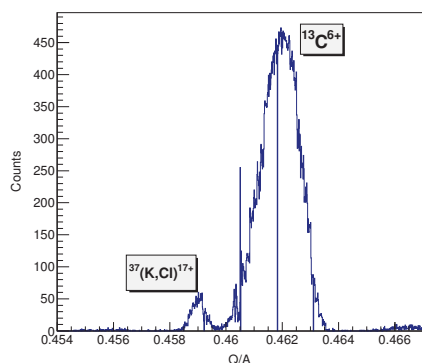

Figure 6: A projection of the matrix shown in Fig. 5 on to the Q/A axis showing the separation of the $^{13}C^{6+}$ peak from the peak corresponding to $^{37}(K,Cl)^{17+}$.

The beam was finally transported to the ANASEN (Array for Nuclear Astrophysics Studies with Exotic Nuclei) to observe the excitation function of the $^{37}K(p,p)$ reaction. Following the reaction within this device, the heavy projectile is incident upon a segmented anode ionization chamber. Figure 7 shows two dimensional PID plots of the energy in the first segment (delta-E) versus total energy in all segments, in arbitrary units. This figure is provided courtesy of the ANASEN collaboration. The top panel shows the PID without injection of the ^{37}K into the EBIT, and the bottom panel with injection. The separation of ^{13}C from ^{37}K is evident, and it was for this reason that $^{37}K^{17+}$ was chosen for transport to the experiment. The background rate of ^{37}Cl was relatively low and sufficiently separated from the ^{37}K to not impair the measurement.
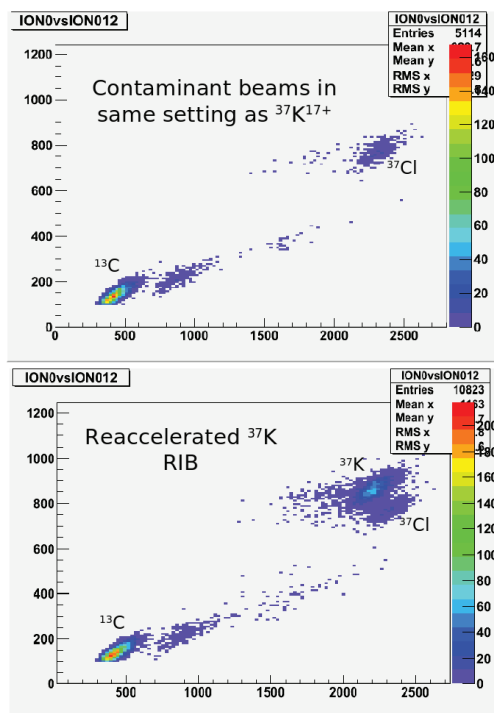

Figure 7: Two dimensional Particle ID plots of delta-E versus E in the ANASEN ionchamber. Upper panel: ^{37}K EBIT injection off. Lower panel:^{37}K EBIT injection on.

CONCLUSION

Beams of ^{76}Ga and ^{37}K were successfully thermalized and reaccelerated for the first time in two commissioning experiments recently performed at the National Superconducting Cyclotron Laboratory. The diagnostics challenges facing this technique were discussed in detail with emphasis been given to the diagnostics of the rare isotope beams. The authors would like to thank the ANASEN collaboration at Louisiana State University and Florida State University for their contribution. This work is supported by Michigan State University and the US National Science Foundation.

REFERENCES

[1] D. Leitner, *et al.*, Proceedings of SRF2011, Chicago, IL, USA, 2011, THIOB03

[2] D. J. Morrissey, "The Coupled Cyclotron Project at the NSCL," Nuclear Physics **A 616** (1997) 45055

[3] M. Leitner, *et al.*, Proceedings of SRF2011, Chicago, IL, USA, (2011), MOPO009, p. 56

[4] D. J. Morrissey, B. M. Sherrill, M. Steiner, A. Stolz, and I. Wiedenhoever, Nucl. Instrum. Methods Phys. Res., Sect. **B 204**, 90 (2003).

[5] L. Weissman, *et al.*, Nucl. Phys. **A 746** (2004) 655.

[6] G. Savard, J. Phys. Conf. Ser. 312 (2011) 052004.

[7] A. Lapierre, *et al.*, AIP Conf. Proc. **1525** 497 (2013)